2010 IEEE International Conference on Robotics and Automation
Anchorage Convention District
May 3-8, 2010, Anchorage, Alaska, USA

A Discrete-Time Filter for the On-Line Generation of Trajectories with Bounded Velocity, Acceleration, and Jerk

Oscar Gerelli and Corrado Guarino Lo Bianco, *IEEE Member*

***Abstract*— The performances of controlled systems can be improved by driving them with smooth reference signals. In case of rough signals, smoothness can be achieved with the help of appropriate dynamic filters. To this purpose a novel discrete-time filter is proposed in the paper. It has been appositely designed for real-time motion applications like those that can be encountered in robotic or mechatronic contexts. The filter generates output signals which are continuous together with their first and second time derivatives. Simultaneously, the first, the second, and the third time derivatives are bounded within freely assignable limits. If such limits are changed on-the-fly, the filter hangs the new bounds in minimum-time. An example case shows the filter while tracking steps, ramps and parabolas by means of bounded-dynamic transients.**

I. Introduction

Controllers for robotic and mechatronic applications are commonly driven by means of trajectory generators whose output signals must typically satisfy several requirements [1]. Smoothness is probably the most important: in order to avoid unnecessary mechanical solicitations and to improve the controller performances, the continuity on the position reference signal and on its first derivative, i.e., the velocity, are commonly required.

Other requirements are taken into account as well. For example, the actuators electromechanical limits are often considered by constraining the maximum velocity or acceleration. Furthermore, when possible, also dynamic bounds are accounted for. Trajectories are typically the outcome of off-line algorithms which do not only fulfill the assigned requirements, but also optimize proper performance indexes. A typical robotic application has been proposed by Lin *et al.* in [2]: minimum time trajectories were generated by considering bounds on the joint velocities, accelerations and jerks. Other approaches, like those proposed in [3], [4], also consider the existence of dynamic bounds.

Above mentioned planning techniques, due to their computational burden, can only be applied off-line. As a consequence, if constraints change during transients, replanning must be handled by means of alternative approaches that can be roughly divided into two categories: methods based on decision trees, which efficiently evaluate new feasible trajectories depending on the current system state and on the new constraints [5], [6], [7], [8], and methods based on feedback dynamic systems, which produce feasible trajectories by filtering the originally unfeasible inputs [9], [10]. In all the cases, minimum time transients subject to kinematic constraints are obtained.

This paper proposes an approach based on the latter technique: the filter input and output signals coincide when the formers satisfy the given constraints, otherwise the filter determines new feasible signals which at best emulate the original ones. Continuous-time second-order implementations able to generate outputs which are continuous together with their first derivative, and characterized by bounded velocities and accelerations, were originally considered in [9], [10]. Discrete-time versions, showing similar performances, have been later proposed in [11], [12], [13], [14].

A third-order evolution of the continuous-time filter has been proposed in [15]. It is characterized by the same basic properties of its precursors, but also guarantees continuous acceleration and bounded jerk. Subsequently, a third-order discrete-time version has appeared in [16]. It generates continuous position, velocity, and acceleration signals, but only the jerk is bounded: constraints on the maximum velocity and acceleration are not taken into account.

This paper aims to fill this lacuna. Still in a discrete-time framework, a third-order filter with enhanced capabilities is proposed: it possesses the same characteristics of that described in [16], but it can also handle freely assignable bounds on the velocity and the acceleration.

The paper is organized as follows. In §II the optimal trajectory scaling problem is proposed and solved by means of a new discrete-time filter. The convergence properties of the filter are deeply investigated in §III. A test case is proposed in §IV, while final conclusions are reported in §V.

II. The optimal trajectory scaling problem and the discrete-time filter

The reference-scaling problem considered in this paper is solved by means of a discrete-time filter. In the following, subscript $i \in \mathbb{Z}$ is used to indicate sampled variables acquired at time $t = iT$, where T is the system sampling time. Let us consider the following problem:

Problem 1: Design a nonlinear discrete-time filter whose output x_i tracks at best a given reference signal r_i which is known together with its first and second time derivatives, while $\dddot{r}_i = 0$. The filter must fulfill the following requirements:

1) the first, the second, and the third time derivatives of x_i must be bounded:

$$\dot{x}^- \le \dot{x}_i \le \dot{x}^+, \quad \ddot{x}^- \le \ddot{x}_i \le \ddot{x}^+, \quad -U \le \dddot{x}_i \le U \; , \quad (1)$$

where $\dot{x}^-, \dot{x}^+, \ddot{x}^-, \ddot{x}^+ \in \mathbb{R}$, and $U \in \mathbb{R}^+$.

This work is supported in part by the AER-TECH LAB, Emilia Romagna, Italy

The authors are with the Dip. di Ing. dell'Informazione, University of Parma, Italy, email: {guarino,gerelli}@ce.unipr.it

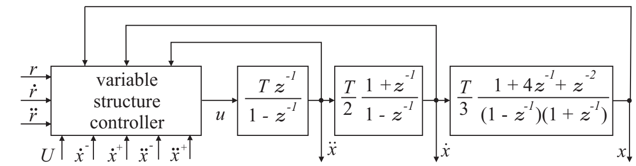

Fig. 1. The discrete-time system which solves *Problem 1*. The system is composed by a dynamic chain based on three integrators and an algebraic variable structure controller.

2) bounds (1) can be time-varying and can also change during transients;
3) if (1) are not satisfied, due to the filter initial conditions or to a sudden change of the bounds, $\dddot{x}_i$ must be forced in a single step within the given limits, while $\dot{x}_i$ and $\ddot{x}_i$ must reach the assigned bounds in minimum time;
4) when a reference signal r_i satisfying (1) is applied, the tracking condition $x_i = r_i$ is reached in minimum time and, compatibly with (1), without overshoot;
5) when a discontinuous reference signal is applied (or the reference signal has time derivatives larger than the bound values), the tracking is lost. As soon as the reference signal newly satisfies (1), tracking is achieved in minimum time;
6) the time derivatives $\dot{x}_i$, $\ddot{x}_i$, and $\dddot{x}_i$ of bounded output x_i must be available for the generation of feedforward actions.

The solution of *Problem 1* represents an interesting challenge: an optimal minimum-time reference tracking problem subject to constraints on the output dynamics. Roughly speaking, given a reference r_i, which could possibly not fulfill bounds (1), the filter must generate a feasible output x_i which tracks r_i at best, compatibly with the constraints. This implies that feasibility is a priority for the filter, so that r_i is voluntarily lost any time it becomes unfeasible. It is worth noticing that constraints on the maximum velocity and acceleration could also be asymmetric.

The solution proposed in the following is based on a discrete time filter whose scheme is shown in Fig. 1. It is made of a chain of three integrators driven by an algebraic control law (ACL). The filter outputs coincide with the filter states x_i, $\dot{x}_i$, and $\ddot{x}_i$.

The integrators' chain can be posed into a state-space form leading to the following discrete-time system

$$\mathbf{x}_{i+1} = \mathbf{A}\,\mathbf{x}_i + \mathbf{b}\,u_i\,, \tag{2}$$

where

$$\mathbf{A} = \begin{bmatrix} 1 & T & \frac{T^2}{2} \\ 0 & 1 & T \\ 0 & 0 & 1 \end{bmatrix}, \quad \mathbf{b} = \begin{bmatrix} \frac{T^3}{6} \\ \frac{T^2}{2} \\ T \end{bmatrix}, \tag{3}$$

and $\mathbf{x}_i := [x_i\ \dot{x}_i\ \ddot{x}_i]^T$ is the system state.

The hypothesis $\dddot{r}_i = 0$ implies that reference signal r_i can be a constant, a ramp or a parabola. Indeed, due to such hypothesis, r_i generally evolves like a parabola according to the following expressions

$$\dddot{r}_{i+1} := 0\,, \tag{4}$$
$$\ddot{r}_{i+1} := \ddot{r}_i\,, \tag{5}$$
$$\dot{r}_{i+1} := \dot{r}_i + T\ddot{r}_i\,, \tag{6}$$
$$r_{i+1} := r_i + T\dot{r}_i + \frac{T^2}{2}\ddot{r}_i\,, \tag{7}$$

but a linear trend can be achieved by further imposing $\ddot{r}_i = 0$ or, finally, a constant signal is obtained if also $\dot{r}_i = 0$.

Consider the following change of coordinates $y_i := x_i - r_i$, $\dot{y}_i := \dot{x}_i - \dot{r}_i$, $\ddot{y}_i := \ddot{x}_i - \ddot{r}_i$, which allocates the system origin on the trajectory to be tracked. Due to the change of coordinates, and bearing in mind (4)–(7), system (2) becomes

$$\mathbf{y}_{i+1} = \mathbf{A}\,\mathbf{y}_i + \mathbf{b}\,u_i\,, \tag{8}$$

where $\mathbf{A}$ and $\mathbf{b}$ coincide with (3), while $\mathbf{y}_i := [y_i\ \dot{y}_i\ \ddot{y}_i]^T$.

Matrices $\mathbf{A}$ and $\mathbf{b}$ depend on sampling time T. In order to drop such dependence, a further transformation $\mathbf{y}_i = \mathbf{W}\,\mathbf{z}_i$ is proposed, where

$$\mathbf{W} = TU \begin{bmatrix} T^2 & -T^2 & \frac{T^2}{6} \\ 0 & T & -\frac{T}{2} \\ 0 & 0 & 1 \end{bmatrix}, \tag{9}$$

and $\mathbf{z}_i := [z_{1,i}\ z_{2,i}\ z_{3,i}]^T$. The transformed system is

$$\mathbf{z}_{i+1} = \mathbf{A}_d\,\mathbf{z}_i + \mathbf{b}_d\,u_i\,, \tag{10}$$

with

$$\mathbf{A}_d = \begin{bmatrix} 1 & 1 & 1 \\ 0 & 1 & 1 \\ 0 & 0 & 1 \end{bmatrix}, \quad \mathbf{b}_d = \frac{1}{U}\begin{bmatrix} 1 \\ 1 \\ 1 \end{bmatrix}. \tag{11}$$

Matrix $\mathbf{W}$ is non singular, so that the inverse transformation $\mathbf{z}_i = \mathbf{W}^{-1}\,\mathbf{y}_i$ exists with

$$\mathbf{W}^{-1} = \frac{1}{TU}\begin{bmatrix} \frac{1}{T^2} & \frac{1}{T} & \frac{1}{3} \\ 0 & \frac{1}{T} & \frac{1}{2} \\ 0 & 0 & 1 \end{bmatrix}. \tag{12}$$

The solution proposed in this paper for *Problem 1* is obtained by driving (2) with the following ACL (subscript i has been dropped for conciseness):

$$z_2^+ := \frac{\dot{x}^+ - \dot{r}}{T^2U}\,, \tag{13}$$

$$z_2^- := \frac{\dot{x}^- - \dot{r}}{T^2U}\,, \tag{14}$$

$$z_3^+ := \frac{\ddot{x}^+ - \ddot{r}}{TU}\,, \tag{15}$$

$$z_3^- := \frac{\ddot{x}^- - \ddot{r}}{TU}\,, \tag{16}$$

$$\overline{z}_2^+ := -\lceil z_3^+ \rceil \left[z_3^+ - \frac{\lceil z_3^+ \rceil - 1}{2} \right], \tag{17}$$

$$\overline{z}_2^- := \lceil -z_3^- \rceil \left[-z_3^- - \frac{\lceil -z_3^- \rceil - 1}{2} \right], \tag{18}$$

$$d_1 := z_2 - z_2^+\,, \tag{19}$$

$$d_2 := z_2 - z_2^- \ , \tag{20}$$

for n=1,2:

$$\gamma_n := \begin{cases} \bar{z}_2^+ & \text{if } d_n < \bar{z}_2^+ \\ d_n & \text{if } \bar{z}_2^+ \le d_n \le \bar{z}_2^- \\ \bar{z}_2^- & \text{if } d_n > \bar{z}_2^- \end{cases} \ , \tag{21}$$

$$m_n := \left\lfloor \frac{1+\sqrt{1+8\,|\gamma_n|}}{2} \right\rfloor \ , \tag{22}$$

$$\sigma_n := -\frac{m_n - 1}{2}\operatorname{sgn}(\gamma_n) - \frac{\gamma_n}{m_n} \ , \tag{23}$$

end for

$$\begin{aligned} \sigma_3 \quad := \quad & -\frac{2h+k-1}{h(h+k)} z_2 - \frac{2}{h(h+k)} z_1 \\ & -\frac{2h^3+k^3+3h^2k-3hk-3h^2+h-k}{6h(h+k)}\eta \ , \end{aligned} \tag{24}$$

$$\sigma := \begin{cases} \sigma_1 & \text{if} \quad \sigma_1 < \sigma_3 \\ \sigma_3 & \text{if} \quad \sigma_2 \le \sigma_3 \le \sigma_1 \\ \sigma_2 & \text{if} \quad \sigma_3 < \sigma_2 \end{cases} \ , \tag{25}$$

$$\alpha := z_3 - \sigma \ , \tag{26}$$

$$u := -U \operatorname{sat}(\alpha) \ , \tag{27}$$

where z_1, z_2 and z_3 are obtained by means of (12), while integers h, k, and η are functions of z_1 and z_2. For details on h, k, and η the interested reader can refer to [16]. In the next section the ACL characteristics will be deeply analyzed and, in particular, it will be proved that it solves *Problem 1* given that $z_2^+, z_3^+ \in \mathbb{R}^+$ and $z_2^-, z_3^- \in \mathbb{R}^-$. The two operators $\lfloor\cdot\rfloor$ and $\lceil\cdot\rceil$ respectively evaluate the floor and the ceil of a real number. Function $\operatorname{sat}(\cdot)$ saturates its argument to ± 1.

The ACL is a variable structure controller [17] which switches among three different sliding-mode controllers depending on the current system state. Associated with each controller is one of the three sliding surfaces (SSs) σ_1, σ_2, and σ_3 with its corresponding boundary layer (BL). It is evident from (19)–(23) that σ_1 and σ_2 only depend on z_2: functions $\sigma_1(z_2)$ and $\sigma_2(z_2)$ are shown in Figs. 2a and 2b respectively, together with the corresponding system trajectories. Conversely, due to (24), surface σ_3 depends on both z_1 and z_2. As a consequence, the position of σ_3 is not constant when projected onto the (z_2, z_3)-plane: given z_2, it is possible to have several values of σ_3 depending on z_1, as evidenced by Fig. 3. Surface σ_3 is the same proposed in [16] and guarantees the optimal minimum-time convergence toward the origin in absence of constraints on the velocity and acceleration. In this paper, the attention is mainly focused on σ_1 and σ_2, which are appositely introduced to fulfill the velocity and the acceleration constraints.

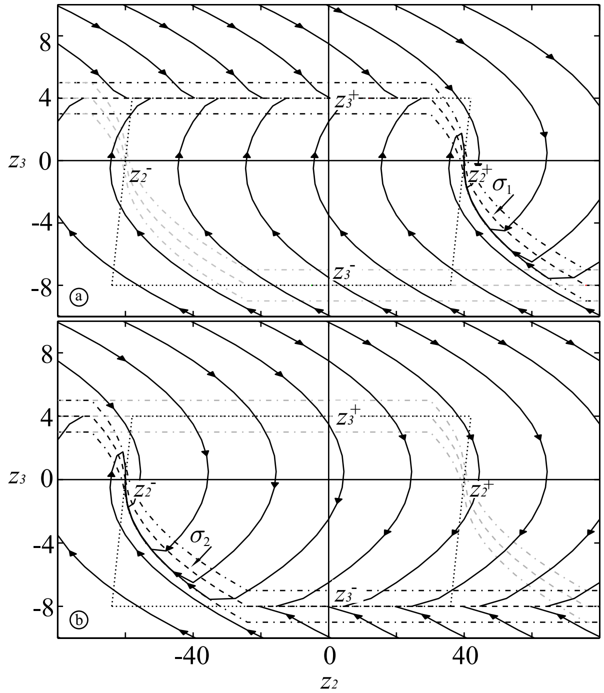

Fig. 2. System trajectories in the (z_2, z_3) phase plane for $\sigma = \sigma_1$ (figure a) and for $\sigma = \sigma_2$ (figure b). SSs σ_1 and σ_2 are indicated by means of dashed lines and are surrounded by their BLs (dash dotted lines). The dotted quadrangle contours the feasible area.

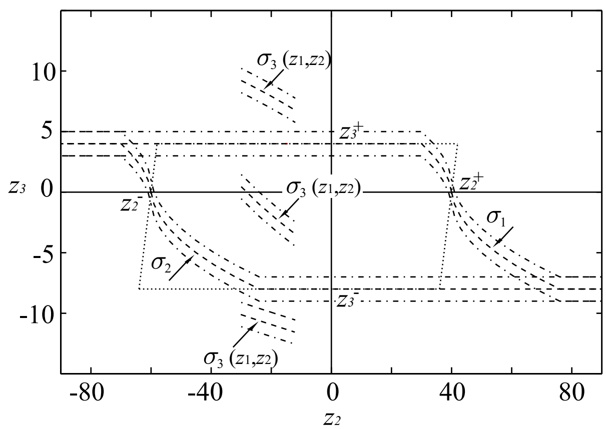

Fig. 3. The three SSs σ_1, σ_2, and σ_3 which characterize the filter ACL. The projection of σ_3 on the (z_2, z_3)-plane depends on the current value of z_1: three different cases are shown for $z_2 = -20$ and $z_1 = 1500, 150, -100$.

III. The filter convergence properties

Some preliminary considerations are instrumental to better understand the filter behavior. Velocity bounds $\dot{x}^-, \dot{x}^+$ and acceleration bounds $\ddot{x}^-, \ddot{x}^+$ can be converted into constraints on $\dot{y}$ and $\ddot{y}$ according to $\dot{y}^+ := \dot{x}^+ - \dot{r}$, $\dot{y}^- := \dot{x}^- - \dot{r}$, $\ddot{y}^+ := \ddot{x}^+ - \ddot{r}$, $\ddot{y}^- := \ddot{x}^- - \ddot{r}$. Subsequently, such constraints are transformed by means of (12) into equivalent bounds surrounding the feasible area in the (z_2, z_3)-plane. Bearing in mind (13)-(16), such bounds can be expressed as follows: $z_3 = z_3^+$; $z_3 = z_3^-$; $z_2 - \frac{z_3}{2} = z_2^+$; $z_2 - \frac{z_3}{2} = z_2^-$. The feasible zone is highlighted in Figs. 2, 3, and 4 by means of a dotted quadrangle: until the state remains inside the quadrangle, velocity and acceleration constraints are fulfilled. The control laws associated with σ_1

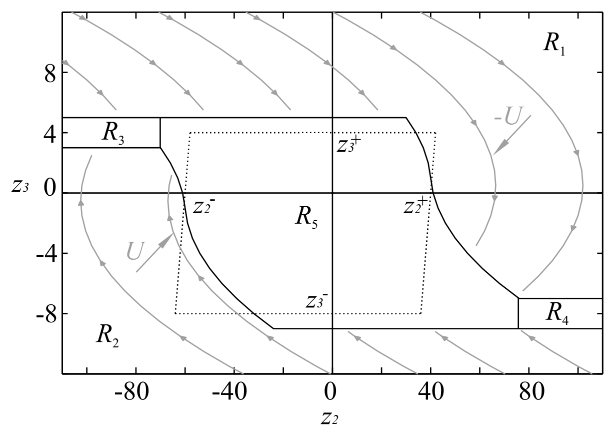

Fig. 4. Partitions induced in the (z_2, z_3)-plane by the ACL.

and σ_2 are designed to force the system, in minimum-time, inside the feasible area. It is worth noting that such area is independent from z_1, and for this reason the discussion will essentially focus on the system behavior on the (z_2, z_3)-plane.

The system evolution in the (z_2, z_3)-plane can be deduced from (10) and (11)

$$\begin{bmatrix} z_{2,i+1} \\ z_{3,i+1} \end{bmatrix} = \begin{bmatrix} 1 & 1 \\ 0 & 1 \end{bmatrix} \begin{bmatrix} z_{2,i} \\ z_{3,i} \end{bmatrix} + \frac{1}{U} \begin{bmatrix} 1 \\ 1 \end{bmatrix} u_i \,. \tag{28}$$

It is straightforward to verify that the system dynamics coincides with that of the system considered in [11], [12], with the sole difference that the role of the pair z_1 and z_2 is now played by z_2 and z_3, while the role of y and $\dot{y}$ is played by $\dot{y}$ and $\ddot{y}$. σ_1 and σ_2 are similar to the SS proposed in [12], but σ_1 is obtained by right shifting the original SS by z_2^+, while σ_2 is obtained through a left shift equal to z_2^-.

Let us subdivide the (z_2, z_3)-plane into the five regions R_i, $i = 1, 2, \ldots, 5$ shown in Fig. 4.

Property 1: For any point (z_2, z_3) lying in $R1$, the ACL returns $u = -U$. Conversely, for any point (z_2, z_3) lying in $R2$, the ACL returns $u = U$.

Proof: Let us suppose that point (z_2, z_3) is lying in $R1$. Three cases could arise depending on the relationship occurring between σ_1, σ_2, and σ_3. If $\sigma_3(z_1, z_2) > \sigma_1(z_2)$, due to (25) the SS is $\sigma = \sigma_1(z_2)$. Since point (z_2, z_3) is outside the BL and $z_3 > \sigma$, (26) and (27) return $u = -U$. Similarly, if $\sigma_1(z_2) \geq \sigma_3(z_1, z_2) \geq \sigma_2(z_2)$ then the SS is $\sigma = \sigma_3(z_1, z_2)$. Even in this case the point is located outside the BL, so that $\alpha > 1$ and, in turn, $u = -U$. Finally, also when $\sigma = \sigma_2(z_2)$ the situation does not change: $\alpha > 1$ and $u = -U$.

Similar considerations hold if (z_2, z_3) is initially located in $R2$: in this case the command signal becomes $u = U$. ■

Remark 1: Property 1 asserts that the maximum command is always applied in $R1$ and $R2$, so that trajectories are shaped as shown in Fig. 4 and the system converges in minimum time toward one of the regions $R3$, $R4$, and $R5$. As a consequence, the area where the acceleration constraint is satisfied, i.e., $z_3^- \leq z_3 \leq z_3^+$, is reached in minimum-time.

Property 2: Any point (z_2, z_3) lying in $R3$, is forced in a single step on σ_1 and then it slides toward $R5$ with command signal $u = 0$. Conversely, any point in $R4$ is forced in a single step on σ_2 and then it slides toward $R5$ with $u = 0$.

Proof: Consider a point (z_2, z_3) belonging to $R3$. Region $R3$ coincides with the common BL of σ_1 and σ_2. It is easy to verify that in such region (25) always returns, independently from the position of σ_3, $\sigma = \sigma_1 = \sigma_2 = z_3^+ \geq 0$. According to (28), z_3 evolves as follows

$$z_{3,i+1} = z_{3,i} + \frac{u_i}{U} \,. \tag{29}$$

Due to (26) and (27), the command signal is $u_i = -U(z_{3,i} - \sigma_{1,i}) = -U(z_{3,i} - z_3^+)$, so that (29) returns $z_{3,i+1} = z_3^+$ independently from $z_{3,i}$, i.e., the SS is reached in a single step. Successively, u becomes equal to zero since the point lyes on the SS and, again due to (29), z_3 remains constant and positive. The evolution of z_2 can be deduced from (28) as well and, in particular, it is equal to

$$z_{2,i+1} = z_{2,i} + z_{3,i} + \frac{u_i}{U} \,. \tag{30}$$

For any point lying on the SS $u_i = 0$ and $z_{3,i} = z_3^+$, so that $z_{2,i+1} = z_{2,i} + z_3^+$, i.e., z_2 slides right with increments equal to z_3^+.

A similar transient occurs in $R4$ but, due to symmetry, the state slides left. ■

Remark 2: Property 2 asserts that if the system enters in $R3$ or in $R4$, it is "captured" and pushed toward $R5$. The constraint on the maximum acceleration is not violated since $z_3 = z_3^+$ in $R3$, while $z_3 = z_3^-$ in $R4$. In any case, the movement along z_2 occurs with the maximum admissible acceleration and, consequently, $R5$ is reached in minimum time.

Therefore, due to Properties 1 and 2 and independently from the initial conditions, the state reaches with certainty region $R5$ with the minimum number of steps and compatibly with the assigned constraints. Next properties will show that the state cannot abandon region $R5$ once it has been reached and, furthermore, it converges toward the origin.

The system evolution of any point lying in $R5$ depends, due to (25), on the relationship existing between the SSs.

Property 3: Consider a starting point (z_2, z_3) belonging to $R5$. The system remains inside $R5$ and converges toward the origin or one of the two points $\left(z_2^-, 0\right)$, $\left(z_2^+, 0\right)$.

Proof: Three cases could arise depending on σ_3.

- Case $\sigma_3(z_1, z_2) > \sigma_1(z_2)$

The SS, according to (25), is σ_1. Trajectories within $R5$ assume the shape shown in Fig. 2a. It is evident that all the trajectories starting from points located inside $R5$ remain inside that region and converge toward σ_1. With the same reasonings reported in [12], it is possible to prove that the state first joins the BL of σ_1 and then it slides toward $\left(z_2^+, 0\right)$, which is reached in minimum-time compatibly with the constraint on z_3.

- Case $\sigma_3(z_1, z_2) < \sigma_2(z_2)$

The situation is similar to the previouos one but, according to Fig. 2b, the system is first attracted by σ_2 and then it slides toward $\left(z_2^-, 0\right)$.

- Case $\sigma_2(z_2) \leq \sigma_3(z_1, z_2) \leq \sigma_1(z_2)$

The SS, according to (25), is σ_3. It is worth remembering that σ_3 is designed to force the system toward the origin in minimum-time. Differently from the other two SSs, σ_3 could

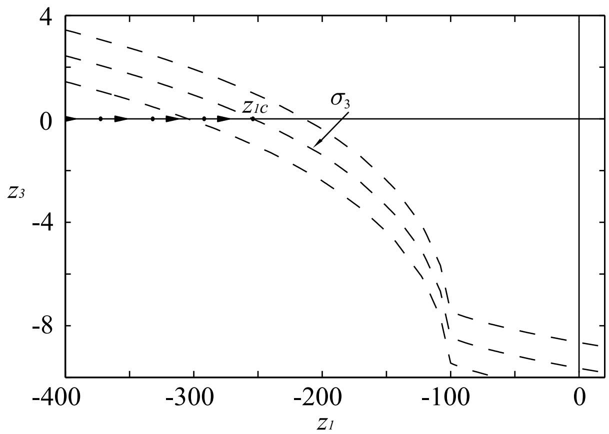

Fig. 5. Surface σ_3 and its BL drawn for $z_2 = z_2^+ = 40$. The system transient along the z_1 axis is highlighted by means of arrows and dots.

abandon $R5$, consequently driving the system state outside the feasible zone: immediately the ACL switches to surface σ_1 or σ_2, so that the state remains inside $R5$. ■

The ACL strategy inside $R5$ can be easily explained. Surface σ_3 forces the system toward the origin in minimum-time. Consequently, inside R5, σ_3 is the preferred SS unless it would drive the system outside the feasible area. In such eventuality, the state is "parked" in $\left(z_2^-, 0\right)$ or $\left(z_2^+, 0\right)$, which are both feasible, waiting until σ_3 newly enters region $R5$.

Property 4: The two points $\left(z_2^-, 0\right)$ and $\left(z_2^+, 0\right)$ are left with certainty in finite time.

Proof: Let us first suppose that $\sigma_3 > \sigma_1$. Bearing in mind *Property 3*, it is possible to assert that the system converges to $\left(z_2^+, 0\right)$, which lays on σ_1, and by virtue of (27) we have $u = 0$. Once $\left(z_2^+, 0\right)$ has been reached, due to (10) and (11) the system evolves as follows

$$z_{3,i+1} = z_{3,i} = 0\,, \tag{31}$$

$$z_{2,i+1} = z_{2,i} + z_{3,i} = z_2^+\,, \tag{32}$$

$$z_{1,i+1} = z_{1,i} + z_{2,i} + z_{3,i} = z_{1,i} + z_2^+\,, \tag{33}$$

i.e., owing to (31) and (32) it remains in $\left(z_2^+, 0\right)$, but, in the meanwhile, according to (33), z_1 increases with steps equal to $z_2^+ > 0$. The system behaviour can be better understood by observing the phase plane from a different point of view. Fig. 5 shows the trend of σ_3 in the (z_1, z_3)-plane when $z_2 = z_2^+$. The figure highlights that σ_3 is a monotonically decreasing function of z_1. This is a structural characteristic of σ_3, which applies for any value of z_2. In $\left(z_2^+, 0\right)$, $\sigma_1 = 0$, which implies that $\sigma_3 > 0$, being $\sigma_3 > \sigma_1$. A consequence of the σ_3 positivity is that the current value of z_1 is certainly located on the left of z_{1c}, where z_{1c} is the solution of the equation $\sigma_3(z_1, z_2^+) = 0$ (see also Fig. 5). Due to (33), z_1 increases at the maximum velocity allowed by the feasibility conditions and the corresponding value of σ_3 decreases. As soon as σ_3 becomes negative the control law switches, the convergence point $(z_2^+, 0)$ is abandoned and the system starts following σ_3 with control law $u = -U$ [16].

Analogous considerations hold when $\sigma_3 < \sigma_2$ and the system is initially locked in $\left(z_2^-, 0\right)$. ■

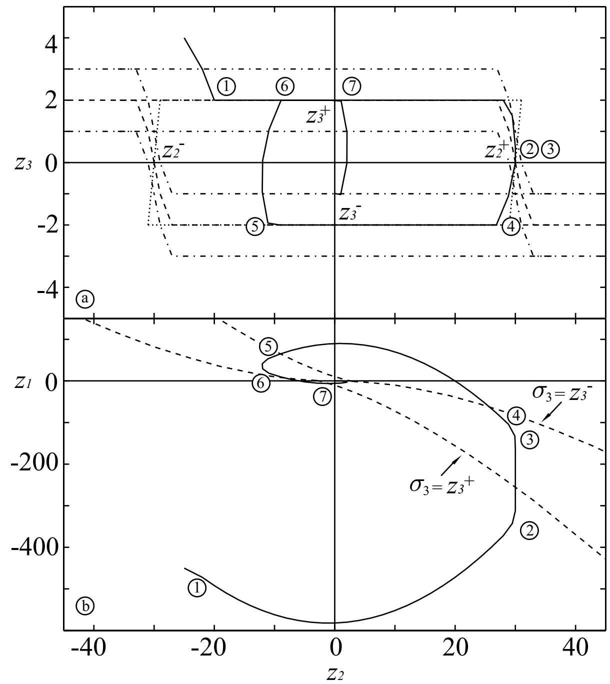

Fig. 6. Details of the system trajectories inside R5. a) state transient in the (z_2, z_3)-plane; b) state transient in the (z_2, z_1)-plane (solid line) and isolines corresponding to $\sigma_3 = z_3^+$ and $\sigma_3 = z_3^-$ (dashed line).

After σ_3 has been hanged, and $\left(z_2^+, 0\right)$ [or $(z_2^-, 0)$] has been left, two situations can occur. In the first case the state trajectory obtained by tracking σ_3 completely belongs to the feasible area and the system is driven in minimum time toward the origin. In the second case the trajectory tends to violate the acceleration bound, so that the ACL newly switches to σ_2 (or to σ_1) in order to preserve the feasibility.

The system behaviour inside $R5$ can be understood with the help of Fig. 6. In particular, Fig. 6a refers to an example state transient in the (z_2, z_3)-plane, while Fig. 6b shows the same transient in the (z_1, z_2)-plane and, with dashed curves, the isolines corresponding to $\sigma_3 = z_3^+$ and $\sigma_3 = z_3^-$. In correspondence with the starting point $\sigma_3 > \sigma_1$, so that the SS is $\sigma = \sigma_1$ and the system is forced inside the feasible area in minimum time (point 1). Then, the system evolves in the (z_2, z_1)-plane with a parabolic trend. After a finite number of steps, point $(z_2^+, 0)$ in the (z_2, z_3)-plane is reached and hanged (point 2). From that moment, in the (z_2, z_1)-plane the system travels vertically pointing at σ_3 at the maximum speed allowed by the constraints. When the unlocking condition is satisfied (point 3), the system starts following σ_3, which is suddenly abandoned for σ_2 in order to avoid violating the acceleration constraint z_3^- (point 4). A new parabolic trajectory occurs in the (z_2, z_1)-plane. This time σ_3 is reached before the velocity saturates (point 5), but it is newly abandoned (point 6) due the acceleration constraint. Again, a parabolic trajectory starts in the (z_2, z_1)-plane, until a new intersection with σ_3 occurs (point 7). The final trajectory obtained following σ_3 does not more violate any constraint, so that the system is driven toward the origin with no further commutations. A formal proof of the convergence toward the origin is omitted for conciseness.

IV. A TEST CASE

The proposed filter has been tested by means of a discontinuous signal made of a step, a ramp and a parabola. Kinematic bounds have been taken into account by initially assuming $\dot{x}^+ = 0.65$, $\dot{x}^- = -1$, $\ddot{x}^+ = 1.6$, $\ddot{x}^- = -2$, $U = 5$. Fig. 7 shows a comparison between the original rough signal and the filter output: x tracks at best reference r, compatibly with the given constraints, which are never exceeded. Fig. 7 also shows that a $t = 1.2$ s, the filter bounds are changed as follows: $\dot{x}^+ = 0.56$, $\dot{x}^- = -1$, $\ddot{x}^+ = 1.3$, $\ddot{x}^- = -1.8$, $U = 7$. As required, jerk constraint is immediately recovered, while acceleration and velocity constraints are newly satisfied in minimum-time compatibly with the jerk constraint itself.

One remark concerns the possible presence of overshoots at the end of an hanging transient. Every time constraints $\dot{x}^+$, $\dot{x}^-$, $\ddot{x}^+$, $\ddot{x}^-$ are touched the minimum-time sliding surface σ_3 is lost: the system cannot be driven toward the origin until σ_3 is newly reached. If σ_3 is lost during the final transient toward r, an overshoot will appear. This property also characterizes the continuous-time filter proposed in [15]. Very stringent values for $\dot{x}^+$, $\dot{x}^-$, $\ddot{x}^+$, $\ddot{x}^-$ have been selected for the example case in order to highlight these overshoots.

A second problem could arise if r is not hanged with a deadbeat approach: overshoots could appear even when saturations are not involved, and the jerk signal could chatter after the reference signal has been reached. The proposed filter is not affected by this problems, which conversely could influence, e.g., the filter in [1] obtained by discretizing [15].

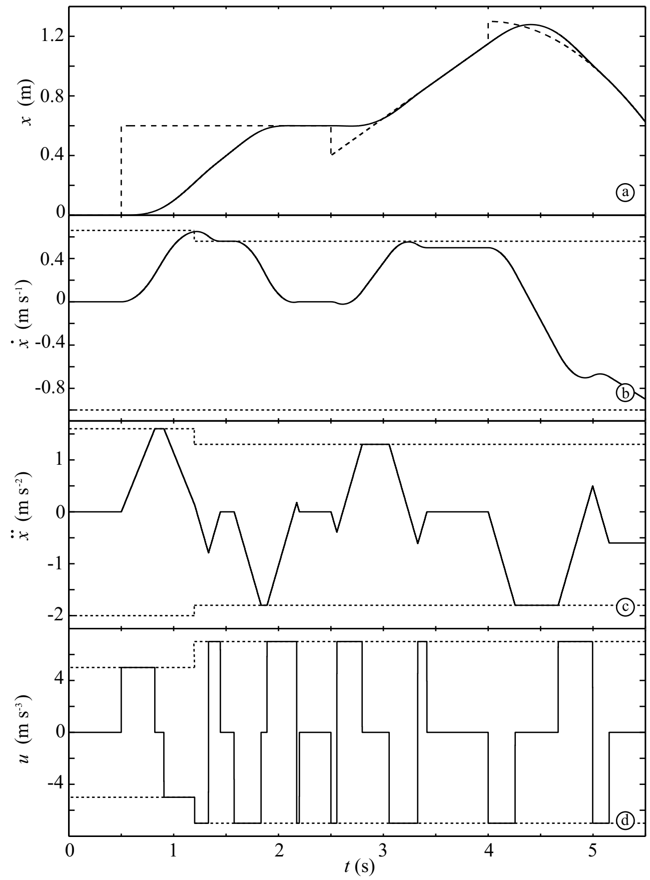

Fig. 7. The simulated test case: a) the non-smooth reference signal (dashed lines) is compared with the filter output; b) the filter velocity signal; c) the filter acceleration signal; d) the filter jerk signal.

V. CONCLUSIONS

The discrete-time filter proposed in the paper is able to generate smooth reference signal which tracks at the best rough inputs, while fulfilling assigned kinematic constraints. The proposed filter enhances the performances of analogous schemes proposed in the literature since it takes into account, for the first time in a discrete-time context, the existence of bounds on the first and the second time derivatives. The filter is suited for motion control applications which require the online generation of smooth trajectories.

REFERENCES

[1] L. Biagiotti and C. Melchiorri, *Trajectory Planning for Automatic Machines and Robots*, first edition ed. Heidelberg, Germany: Springer, Berlin, 2008.

[2] C.-S. Lin, P.-R. Chang, and J. Luh, "Formulation and optimization of cubic polynomial joint trajectories for industrial robots," *IEEE Trans. Automatic Control*, vol. AC-28, no. 12, pp. 1066–1074, 1983.

[3] A. De Luca, L. Lanari, and G. Oriolo, "A sensitivity approach to optimal spline robot trajectories," *Automatica*, vol. 27, no. 3, pp. 535–539, 1991.

[4] C. Guarino Lo Bianco and A. Piazzi, "Minimum-time trajectory planning of mechanical manipulators under dynamic constraints," *Int. J. of Control*, vol. 75, no. 13, pp. 967–980, 2002.

[5] S. Liu, "An on-line reference-trajectory generator for smooth motion of impulse-controlled industrial manipulators," in *Proc. of the seventh Int. Work. on Advanced Motion Control*, 2002, pp. 365–370.

[6] T. Kröger, A. Tomiczek, and F. M. Wahl, "Towards on-line trajectory computation," in *Proc. of the IEEE/RSJ Int. Conf. on Intelligent Robots and Systems, IROS 06*, 2006, pp. 736–741.

[7] R. Haschke, E. Weitnauer, and H. Ritter, "On-line planning of timeoptimal, jerk-limited trajectories," in *Proc. of the IEEE/RSJ Int. Conf. on Intelligent Robots and Systems, IROS 08*, 2008, pp. 3248–3253.

[8] X. Broquère, D. Sidobre, and I. Herrera-Aguilar, "Soft motion trajectory planner for service manipulator robot," in *Proc. of the 2008 IEEE/RSJ Int. Conf. on Intelligent Robots and Systems, IROS 08*, 2008, pp. 2808–2813.

[9] C. Guarino Lo Bianco, A. Tonielli, and R. Zanasi, "Nonlinear trajectory generator," in *IECON96 - 22nd Annual International Conference on the IEEE Industrial Electronics Society*, Taiwan, Taipei, August 1996, pp. 195–201.

[10] R. Zanasi, A. Tonielli, and C. Guarino Lo Bianco, "Nonlinear filter for smooth trajectory generation," in *NOLCOS98 - 4th Nonlinear Control Systems Design Symposium 1998*, vol. 1, Enschede, the Netherlands, July 1998, pp. 245–250.

[11] R. Zanasi, C. Guarino Lo Bianco, and A. Tonielli, "Nonlinear filters for the generation of smooth trajectories," *Automatica*, vol. 36, no. 3, pp. 439–448, March 2000.

[12] C. Guarino Lo Bianco and R. Zanasi, "Smooth profile generation for a tile printing machine," *IEEE Trans. on Ind. Electronics*, vol. 50, no. 3, pp. 471–477, 2003.

[13] X. Wei, J. Wang, and Z. Yang, "Robust smooth-trajectory control of nonlinear servo systems based on neural networks," *IEEE Trans. Industrial Electronics*, vol. 54, no. 1, pp. 208–217, 2007.

[14] O. Gerelli and C. Guarino Lo Bianco, "Real-time path-tracking control of robotic manipulators with bounded torques and torque-derivatives," in *2008 IEEE/RSJ Int. Conf. on Intelligent Robots and Systems, IROS 2008*, Nice, France, Sept. 2008, pp. 532–537.

[15] R. Zanasi and R. Morselli, "Third order trajectory generator satisfying velocity, acceleration and jerk constraints," in *Proc. of the 2002 IEEE Int. Conf. on Control Applications*, Glasgow, Scotland, UK, Sept. 2002, pp. 1165–1170.

[16] ——, "Discrete minimum time tracking problem for a chain of three integrators with bounded input," *Automatica*, vol. 39, no. 9, pp. 1643–1649, 2003.

[17] V. Utkin, "Variable structure systems with sliding modes," *IEEE Transactions on Automatic Control*, vol. 22, pp. 212–222, 1977.